Strained SiGeSn formed by Sn implant into SiGe and pulsed laser annealing

Grace Huiqi Wang and Eng-Huat Toh
Silicon Nano Device Laboratory, Department of Electrical and Computer Engineering, National University of Singapore, Singapore 117576, Singapore

Xincai Wang
Agency for Science, Technology and Research, Singapore Institute of Manufacturing Technology, Singapore 638075, Singapore

Sudhiranjan Tripathy
Agency for Science, Technology and Research, Institute of Materials Research Engineering, Singapore 117602, Singapore

Thomas Osipowicz and Taw Kuei Chan
Center for Ion Beam Applications, Department of Physics, National University of Singapore, Singapore 117542, Singapore

Keat-Mun Hoe, Subramaniam Balakumar, and Guo-Qiang Lo
Agency for Science, Technology and Research, Institute of Microelectronics, 11 Science Park Road, Singapore 117685, Singapore

Ganesh Samudra and Yee-Chia Yeo[a)]
Silicon Nano Device Laboratory, Department of Electrical and Computer Engineering, National University of Singapore, Singapore 11757, Singapore

Incorporation of tin (Sn) in substitutional sites in strained $Si_{0.75}Ge_{0.25}$ was demonstrated by Sn implant and pulsed laser annealing. The surface of $Si_{0.75}Ge_{0.25}$ was amorphized by Sn implant but was recrystallized after pulsed laser annealing. The crystalline $Si_{1-x-y}Ge_xSn_y$ layer formed was studied by Rutherford backscattering spectrometry and Raman spectroscopy. A substitutionality up to 62% Sn and 80% Ge was obtained at an optimal laser power of 400 mJ cm^{-2} for five laser pulses. A compressive strain of -1.15% was also obtained due to Sn incorporation. The presence of Sn also increased the active B dopant concentration in activating $Si_{1-x-y}Ge_xSn_y$ to give low sheet resistance. The implantation of Sn and B followed by pulsed laser annealing could be useful for application in strain engineering of high mobility metal-oxide-semiconductor field-effect transistors. © *2007 American Institute of Physics*. [DOI: 10.1063/1.2803853]

Continued downscaling of complementary metal-oxide-semiconductor (CMOS) transistors faces immense challenges as device miniaturization does not necessarily yield performance enhancement. Therefore, strain-induced effects have been exploited to increase carrier mobility and drive current. Materials such $Si_{1-x}Ge_x$ and $Si_{1-y}C_y$ having a lattice mismatch with Si have been introduced in the source/drain S/D regions of CMOS transistors to induce strain in the channel region.[1,2] Drive current is considerably enhanced in a *p*-channel Si transistor employing SiGe S/D regions due to an increase in hole mobility resulting from a longitudinal compressive strain in the Si channel. This longitudinal compressive strain is induced by the lattice mismatch between SiGe and Si.[3] Higher strain levels in the channel can be achieved by increasing the Ge content in the SiGe S/D stressor or by using S/D materials with an even larger lattice mismatch.[3] SiGeSn can provide a large lattice mismatch with respect to Si, and lead to more pronounced strain effects. Currently, however, there exists no capability for the chemical vapor deposition or epitaxy of SiGeSn.[4–6]

In this letter, we report a technique to form single crystalline SiGeSn by employing ion implantation of Sn in SiGe followed by pulsed laser annealing. Laser annealing is a promising technique that forms ultrashallow junctions with low sheet resistance in CMOS transistors, and has also been effective in repairing crystal damage due to implantation and in achieving high active carrier concentration.[7] We shall also explore the physics behind the compressive strain induced in SiGe due to the presence of Sn, and its effect on the activation of B dopant in SiGeSn. Sn has a very large atomic size (α-Sn a lattice constant of 6.4892 Å) compared to Si and Ge. The covalent radius of the Sn atom is larger than that of SiGe or Si, and its placement in the substitutional site of the host SiGe or Si lattice creates local strain and an increase in the lattice constant.

A compressively strained $Si_{0.75}Ge_{0.25}$ layer with a thickness of 50 nm was pseudomorphically grown on 8 in. *n*-type Si wafers by ultrahigh vacuum chemical vapor deposition. Implant of Sn at an energy of 30 keV and a dose of 8×10^{15} cm^{-2} was performed. The targeted implant depth R_p was 15 nm. The wafer surface, which was amorphized and comprised of $Si_{1-x-y}Ge_xSn_y$, was irradiated with a pulsed XeCl excimer laser with a wavelength λ of 248 nm. Single and multiple laser pulses with varying fluences in the range

a)Author to whom correspondence should be addressed. Tel: +65 6516-2298. FAX: +65 6779-1103. Electronic mail: yeo@ieee.org
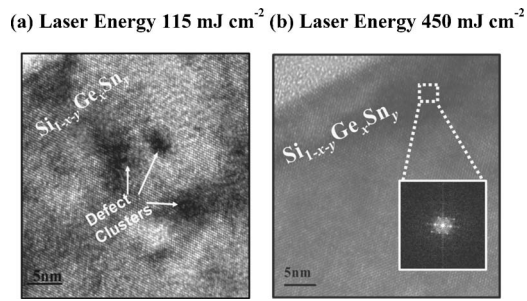
91, 202105-1

(a) Laser Energy 115 mJ cm^{-2} (b) Laser Energy 450 mJ cm^{-2}

FIG. 1. High resolution transmission electron microscopy pictures of a $Si_{1-x-y-z}Ge_xSn_yB_z$ layer on Si substrate after laser annealing. (a) The sample was laser annealed using five laser pulses each with an energy intensity of 115 mJ cm^{-2}. Defect clusters with a size of $\sim 3-5$ nm were observed. (b) With a laser annealing condition of five 400 mJ cm^{-2} pulses, the defect clusters were dissolved, and defect-free single crystalline SiGeSn was formed. This optimized laser annealing condition melted the region with implantation-induced damage and subsequent recrystallation obtained a single crystalline $Si_{1-x-y-z}Ge_xSn_yB_z$ layer.

of 100–600 mJ cm^{-2} were used to study the effect of repeated irradiation on the crystallization and Sn substitutionality in SiGe. An optimized laser energy of 400 mJ cm^{-2} for five pulses produced the least defects among the laser annealing conditions explored, but defect clusters are still found. For another sample with coimplantation of Sn (energy of 30 keV and dose of 8×10^{15} cm^{-2}) and B (energy of 5 keV and dose of 4×10^{15} cm^{-2}), where Sn was implanted before B, denoted as "Sn and B implant," and which was annealed using the same condition of five laser pulses at 400 mJ cm^{-2}, the crystalline structure was recovered when laser annealed at a sufficiently high energy density. No observable defects were seen. We note that when B and Sn implanted samples were laser annealed at lower laser fluence of 115 mJ cm^{-2} for five pulses, small-sized defect clusters of less than 3 nm remained [Fig. 1(a)], but disintegrated at larger laser fluences [Fig. 1(b)]. Generally, with increasing laser fluence, the defect clusters disintegrate and disappear. The incorporation of Sn and B in substitutional sites could lead to reduced strain energy which possibly contributes to reduced defects and better crystalline quality, as compared to samples without B implant. In the absence of B, the formation of a high quality crystalline structure with substantial Sn concentration and high strain levels could be unfavorable.

To quantify the film quality, Rutherford backscatering (RBS) measurements were performed. In subsequent discussion, this paper will focus on Sn and B implanted samples, which form a $Si_{1-x-y-z}Ge_xSn_yB_z$/Si substrate. RBS spectra for laser annealed Sn and B implanted samples are shown in Fig. 2(a). The RBS experiments were carried out using a He$^+$ beam of 2 MeV, detector angle of 160°, and an energy resolution of 16 keV. In Fig. 2(a), the spectra plotted using (i) solid and (ii) dotted lines are the random and channeling spectra, respectively, for the as-implanted $Si_{1-x-y-z}Ge_xSn_yB_z$/Si sample. It can be observed that the random and channeling spectra coincide perfectly, indicating the existence of an amorphized layer prior to laser annealing. Curves labeled (iii) and (iv) are the channeling spectra for samples each annealed with five laser pulses at energy fluence of 115 and 400 mJ cm^{-2} per pulse, respectively. The Sn peak for areas irradiated with five 400 mJ cm^{-2} laser pulses takes the shape of a plateau [line (iv)]. This indicates that the substitutional Sn profile is uniformly distributed within the melted depth of SiGe layer. When laser annealed with five
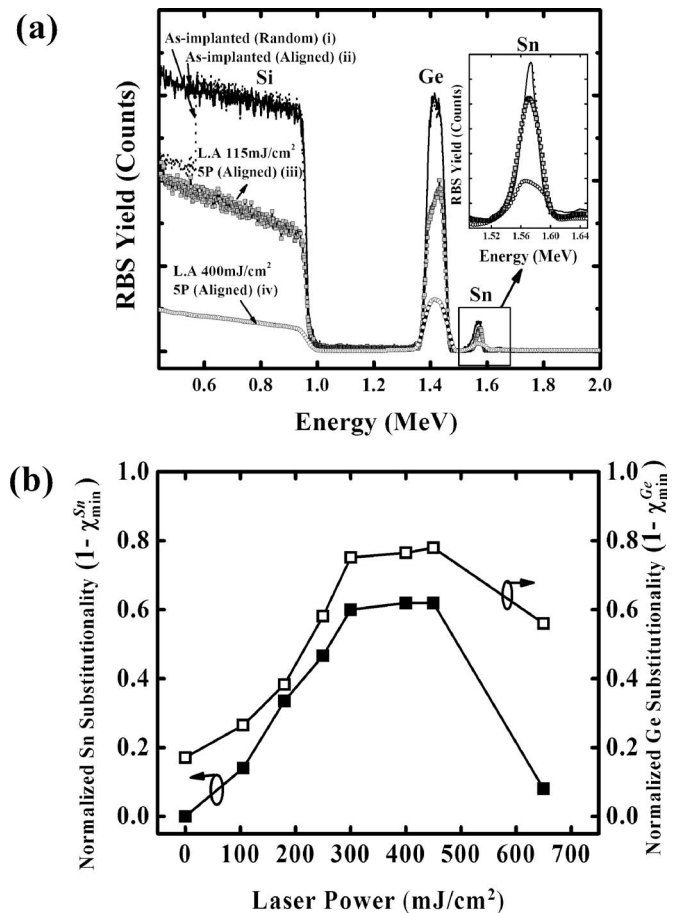

FIG. 2. (a) Rutherford backscattering and channeling spectra for the Sn implanted sample. Spectra plotted using (i) solid and (ii) dotted lines are the random and channeling spectra, respectively, for the as-implanted sample. Lines (iii) and (iv) are the channeling spectra after annealing using five laser pulses each at an energy fluence of 115 and 400 mJ cm^{-2}, respectively. The reduction of the Sn peak (inset) after laser annealing at 400 mJ cm^{-2} for five pulses indicates enhanced Sn substitutionality. Dependence of backscattering yield and substitutional incorporation of (b) Sn and Ge on laser power are investigated. Sn and Ge substitutionality improved, as the laser power was increased from 100 to 400 mJ cm^{-2}. Subsequent increase in laser fluence resulted in significant Sn and Ge drive in, and a reduction in the average concentration of Sn and Ge.

115 mJ cm^{-2} pulses, the Sn peak is higher and closer to the as-implanted peak, as the defects in the $Si_{1-x-y-z}Ge_xSn_yB_z$ layer are not fully eliminated. Hence, a large drop in the Sn peak is desirable. Figure 2(b) shows the backscattering yield of Sn and Ge atoms. Measured dechanneling yield χ_{min} was expressed as the ratio of channeling to random RBS signals. After laser annealing at an optimized condition of 400 mJ cm^{-2} for five pulses, reduction in c_{min} for both the Sn and Ge signals accounted for the substitutional incorporation of 62% Sn and 80% Ge. At higher laser fluences ($>$400 mJ cm^{-2}), a larger extension and distribution of Sn over the melt depth of the $Si_{1-x-y-z}Ge_xSn_yB_z$/Si layer resulted in a reduced concentration of Sn.

Figure 3(a) analyzes the Si–Si and Si–Ge Raman spectra of strained $Si_{1-x-y-z}Ge_xSn_yB_z$/Si before and after laser annealing. The as-grown $Si_{0.75}Ge_{0.25}$ layer was moderately strained (-0.47%). After annealing using fives laser pulses each with an energy density of 250 and 400 mJ cm^{-2}, the characteristic Si–Si peak was shifted from 508.4 to 512.6 and 513.7 cm^{-1}, respectively, indicating a compressive strain of -0.99% and -1.15%, respectively.[8] The incorporation of

(a)

(b)
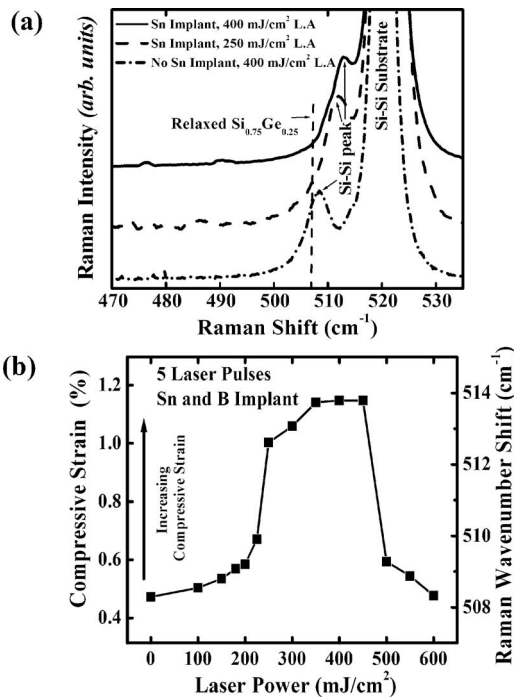

FIG. 3. (a) Raman spectra of $Si_{0.75}Ge_{0.25}$ implanted with Sn and B, followed by laser annealing (LA) with five laser pulses. The Raman shift by 5.3 cm^{-1} to the right was caused by substitutional incorporation of Sn in $Si_{0.75}Ge_{0.25}$, leading to increased in-plane compressive strain. (b) Dependence of Si–Si Raman peak on laser energy density is investigated. Increasing the laser energy density increases the compressive stress in the $Si_{1-x-y-z}Ge_xSn_yB_z$ film due to increased Sn substitutionality.

FIG. 4. Sheet resistance of $Si_{0.75}Ge_{0.25}$ implanted with Sn and B after laser annealing with various energy intensities. Sheet resistance improvement brought about by Sn preamorphization resulted in confinement of boron to a reduced junction depth and a lower sheet resistance was achieved. The diffusion of B at higher laser energy (>400 mJ cm^{-2}) leads to an increase in R_S.

substitutional Sn in $Si_{0.75}Ge_{0.25}$ increased the in-plane compressive strain. We further explore the dependence of laser energy density on the compressive strain induced by Sn in $Si_{0.75}Ge_{0.25}$. Si–Si longitudinal optical phonon peaks are plotted in Fig. 3(b) as a function of laser energy density. Increasing the laser energy from 100 to 400 mJ cm^{-2} increases the in-plane compressive strain in $Si_{0.75}Ge_{0.25}$ from -0.5% to -1.15%. This correlates with increased Sn concentration in $Si_{0.75}Ge_{0.25}$ with laser energy [Fig. 2(b)]. The lattice constant of a $Si_{1-x-y-z}Ge_xSn_yB_z$ alloy can be deduced from Vegard's law.[9] Increasing Sn substitutionality results in an increase in the lattice constant, thereby increasing the Raman frequency for the compressively strained $Si_{1-x-y-z}Ge_xSn_yB_z$. Increasing Sn substitutionality and concentration in the SiGe also results in in-plane compressive stress [Fig. 3(b)], which leads to an increased phonon frequency. This explains the relative right shift in the Si–Si peak.

Figure 4 shows the dependence of sheet resistance R_S of Sn and B implanted layers ($Si_{1-x-y-z}Ge_xSn_yB_z$) on laser anneal energy density. Sn, Ge, and B can diffuse during the laser annealing, and the extent of diffusion increases with the laser energy density and number of laser pulses. With increasing laser energy density, the sheet resistance of B implanted $Si_{0.75}Ge_{0.25}$ (i.e., no Sn) decreases due to higher dopant activation. In the presence of Sn, as-implanted B profile is shallower and more abrupt (as verified from SIMS) due to the absence of channeling. For Sn and B implanted samples, R_S remained lower, in the range of 250–400 mJ cm^{-2}, than samples that only received B implant. We note that the active B concentration is improved in this range of laser energy
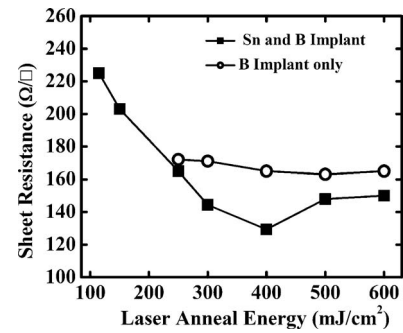
density where Sn substitutionality is improved. In the presence of Sn, activation of B is enhanced,[10] and similar observation has been reported for B activation in the presence of Ge.[11] At higher laser energy (>400 mJ cm^{-2}), significant diffusion of Sn and B occurs, leading to a lower average B concentration, contibuting to a slight increase in R_S.

In conclusion, coimplantation of Sn and B in SiGe/Si substrate followed by laser annealing was demonstrated to form a single crystalline $Si_{1-x-y-z}Ge_xSn_yB_z$ layer. An increase in compressive strain was observed due to incorporation of substitutional Sn. Enhanced activation of B in the presence of Sn was also observed, leading to lower sheet resistance. This work demonstrates a method of fabricating $Si_{1-x-y-z}Ge_xSn_yB_z$ on Si, which could be useful for strain engineering to enhance carrier mobility in advanced metal-oxide-semiconductor field-effect transistors.

[1] Y.-C. Yeo, Semicond. Sci. Technol. **22**, S177 (2007).
[2] G. H. Wang, E.-H. Toh, K. M. Hoe, S. Tripathy, S. Balakumar, G.-Q. Lo, G. Samudra, and Y.-C. Yeo, Tech. Dig. - Int. Electron Devices Meet. **2006**, 469.
[3] Y.-C. Yeo and J. Sun, Appl. Phys. Lett. **86**, 023103 (2005).
[4] S. Y. Shiryaev, J. L. Hansen, P. Kringhoj, and A. N. Larsen, Appl. Phys. Lett. **67**, 2287 (1995).
[5] G. He and H. A. Atwater, Appl. Phys. Lett. **68**, 664 (1996).
[6] F. J. Guarin, S. S. Iyer, A. R. Powell, and B. A. Ek, Appl. Phys. Lett. **68**, 3608 (1996).
[7] J. A. Sharp, N. E. B. Cowern, R. P. Webb, K. J. Kirkby, D. Giubertoni, S. Gennaro, M. Bersani, M. A. Foad, F. Cristiano, and P. F. Fazzini, Appl. Phys. Lett. **89**, 2105 (2006).
[8] Z. Chen, F. Zhang, J. Chen, B. Jin, Y. Wang, C. Zhang, Z. Zhang, and X. Wang, Semicond. Sci. Technol. **20**, 770 (2005).
[9] L. Vegard, Z. Phys. A **5**, 17 (1921).
[10] F. Liu, K.-M. Tan, X. Wang, D. K. Y. Low, D. M. Y. Lai, P. C. Lim, G. Samudra, and Y.-C. Yeo, "Incorporation of the Tin in Boron-Doped Silicon for Reduced Deactivation of Boron During Post-Laser-Anneal Rapid Thermal Processing,"J. Appl. Phys. (to be published).
[11] K. Suzuki, H. Tashiro, K. Narita, and Y. Kataoka, IEEE Trans. Electron Devices **51**, 663 (2004).